Choroidal Caverns: A Novel Optical Coherence Tomography Finding in Geographic Atrophy

Giuseppe Querques,[1,2] Eliana Costanzo,[1] Alexandra Miere,[1] Vittorio Capuano,[1] and Eric H. Souied[1]

[1]Department of Ophthalmology, University Paris Est Creteil, Centre Hospitalier Intercommunal de Creteil, Creteil, France
[2]Department of Ophthalmology, University Scientific Institute San Raffaele, Milan, Italy

Correspondence: Giuseppe Querques, Department of Ophthalmology, University Paris Est Creteil, Centre Hospitalier Intercommunal de Creteil, 40 Avenue de Verdun, 94000 Creteil, France; giuseppe.querques@hotmail.it.

Submitted: January 6, 2016
Accepted: April 15, 2016

Citation: Querques G, Costanzo E, Miere A, Capuano V, Souied EH. Choroidal caverns: a novel optical coherence tomography finding in geographic atrophy. *Invest Ophthalmol Vis Sci*. 2016;57:2578–2582. DOI:10.1167/iovs.16-19083

Purpose. To describe and interpret "choroidal caverns," an unreported optical coherence tomography (OCT) finding in the choroid of patients with geographic atrophy (GA) secondary to atrophic AMD.

Methods. Retrospective analysis of patients with GA. Main outcomes measures included estimation of the prevalence of choroidal caverns, their localization and relation with retinal-choroidal structures by reviewing medical records and multimodal imaging.

Results. One hundred twenty consecutive patients (mean age 80.5 ± 8.61 years) were included. Among the 201 eyes with GA, 17 eyes of 15 patients presented choroidal caverns on OCT B-scan in GA areas (a total of 43 choroidal caverns, mean 2.5/eye, variably localized in the Sattler and Haller layers, with relative preservation of the choriocapillaris). This accounts for 12.5% estimated prevalence (6.5–18.5, 95% confidence interval [CI]) of choroidal caverns in GA areas of atrophic AMD patients. Choroidal caverns appeared on OCT (both B-scan and en face) as gaping hyporeflective cavities in the choroid, typically empty, angular, without hyperreflective borders, often with punctate/linear hyperreflectivities internally. Indocyanine angiography and OCT-Angiography confirmed that the areas occupied by these cavities do not represent perfused choroidal blood vessels.

Conclusions. Choroidal caverns represent a relatively infrequent peculiar finding in GA areas of atrophic AMD eyes. They appear as gaping angular hyporeflective cavities in areas devoid of choroidal vessels, often with punctate/linear hyperreflectivities internally. Choroidal caverns may possibly arise from nonperfused ghost vessels and persistence of stromal pillars where the vessels were originally situated.

Keywords: age-related macular degeneration, choriocapillaris, choroid, en face, fluorescein angiography, geographic atrophy, indocyanine green angiography, infrared, spectral-domain optical coherence tomography, scanning laser ophthalmoscope

Geographic atrophy (GA) represents the late-stage manifestation of atrophic AMD.[1,2] It is defined as a round/oval, sharply demarcated large area (>200 μm) of hypopigmentation with visible choroidal vessels due to loss of retinal pigment epithelium (RPE) and outer retina.[3] It is generally accepted that RPE atrophy and photoreceptor apoptosis are followed by choriocapillaris atrophy.[4–6]

Recent developments in optical coherence tomography (OCT) technologies have enabled the noninvasive in vivo study of the retina and choroid with unprecedented resolution, and thus provided insights into different diseases process including GA.[7–12] Several novel findings have been reported by means of OCT in the retina of GA patients. Zweifel et al.[13] described outer retinal tubulations (ORTs) as branching tubular structures located in the outer nuclear layer (ONL) in a variety of advanced degenerative retinal disorders, including GA.[13] Cohen et al.[14] reported on retinal pseudocysts in atrophic AMD that may correspond to Müller cell degeneration. Our group described wedge-shaped subretinalhyporeflective lesions delimited internally by the hyperreflective outer plexiform layer (OPL) and externally by the hyperreflective Bruch's membrane.[15] Fleckenstein et al.[11] described crown-like elevations in GA areas with presumed debris beneath. Bonnet et al.[16] reported on hyperreflective structures, which the authors suggested to name as "ghost drusen," due to their peculiar appearance and because they develop in GA areas. However, to the best of our knowledge, except for general choroidal thinning,[17–19] no specific findings have been reported by means of OCT in the choroid of GA patients.

Using OCT we observed peculiar findings in the choroid of some atrophic AMD eyes with GA, that we called "choroidal caverns." The purpose of this study is to describe and interpret this previously unreported spectral-domain (SD) OCT finding in GA secondary to atrophic AMD.

Methods

We reviewed the charts of consecutive patients with GA secondary to atrophic AMD that presented at the University Eye Clinic of Creteil (Creteil, France) between January 2012 and December 2014. Inclusion criteria were age greater than 50 years, diagnosis of atrophic AMD with GA defined as any sharply demarcated uni- or multifocal area of absence of the

RPE with visible choroidal vessels larger than 750 μm (diameter). Exclusion criteria were signs of choroidal neovascularization (CNV), intraretinal or subretinal fluid, hemorrhage, subretinal fibrosis, evidence of diabetic retinopathy or any other retinal vascular disease, vitreoretinal disease, myopia greater than 6 diopters (D), any previous treatment (e.g., laser photocoagulation, photodynamic therapy, intravitreal injections of anti-VEGF or steroids), and signs of hereditary retinal dystrophy.

As part of standard clinical assessment, all GA patients underwent best-corrected visual acuity (BCVA) using standard Early Treatment Diabetic Retinopathy Study (ETDRS) charts, slit-lamp examination, fundus biomicroscopy, confocal scanning ophthalmoscope (cSLO) blue fundus autofluorescence (FAF), infrared reflectance (IR), and SD-OCT (Spectralis HRA+OCT; Heidelberg Engineering, Heidelberg, Germany). A subset of patients also underwent cSLO MultiColor imaging, fluorescein angiography (FA), indocyanine green angiography (ICGA), and OCT-Angiography (OCT-A). This study was conducted in accordance with the Declaration of Helsinki for research involving human subjects. Local institutional review board approval was obtained for this study.

Using Spectralis HRA+OCT (Heidelberg Engineering), a standardized imaging protocol was performed in all patients, which included acquisition of cSLO IR reflectance (820 nm; field of view, 30° × 30°; image resolution 768 × 768 pixels) and simultaneous SD-OCT scanning using a second, independent pair of scanning mirrors ($\lambda = 870$ nm; acquisition speed, 40 000 A-scans per seconds; scan depth, 1.8 mm; digital depth resolution, approximately 3.5 μm per pixel; optical depth resolution, 7 μm; lateral optical resolution, 14 μm). The Spectralis software allows averaging a variable number of single images in real time (ART [Automatic Real Time] Module; Heidelberg Engineering) by means of automated eye tracking and image alignment based on cSLO images. The SD-OCT minimum acquisition protocol included 19 horizontal lines, each composed of nine averaged OCT B-scans (1024 A scans per line) at 240-μm intervals, covering a 6 × 6–mm area. Moreover, high-resolution 6 to 9–mm single B-scans (each composed of up to 100 averaged enhanced depth imaging [EDI] OCT B-scans)[9] guided from GA areas, and 25 to 97 sections (each composed of 9 averaged EDI OCT B-scans) at 238- to 28-μm intervals within a 15° × 10° to 20° × 20° rectangle to encompass the GA area, were obtained.

Optical coherence tomography-A examinations were performed by two trained examiners (AM, EC) using the AngioVue XR Avanti (RTVue XR, Optovue, Inc., Freemont, CA, USA), a system previously described in detail allowing obtaining amplitude decorrelation angiography images.[20–22] The system has an A-scan rate of 70,000 scans per second, and uses a light source centered on 840 nm with a bandwidth of 50 nm. To evaluate the morphology, we used a 3 × 3 scanning area. Optical coherence tomography-A volumes consist of 304 × 304 A-scans, each acquired in 3 seconds. Two consecutive B-scans are captured at each fixed position. In order to extract OCTA information, the machine uses split-spectrum amplitude-decorrelation angiography algorithm. During acquisition, motion correction and fixation changes are minimized. The average of the decorrelation values when viewed perpendicularly through the thickness evaluated represent the angiography information. The OCT beam can penetrate to the deep choroid when there is a lack of RPE and choriocapillaris in GA. The automatic segmentation provided by the system software underwent minor manual adjustments, in order to ensure a correct visualization and assessment of the choriocapillaris layer and of the choroidal layers (i.e., Sattler and Haller). A 30-μm section was used from 60 to 90 μm below the RPE for visualizing the Sattler layer and from 90 to 120 μm below the RPE for the Haller layer.

Qualitative descriptions for consecutively collected cSLO (including MultiColor, IR, FA, and ICGA) and OCT (including B-scan, en face and OCT-A) images were performed by two retinal specialists (GQ and EHS). The same retinal specialists also measured the choroidal thickness manually as the distance between the RPE-Bruch's membrane complex and the chorioscleral border at the fovea and at the regions affected by choroidal caverns, and the choroidal caverns greatest linear dimensions and areas on SD-OCT images using the Heidelberg Eye Explorer software (version 1.9.10.0; Heidelberg Engineering). In each study eye, Region Finder (Region Finder, version 2.5.8.0; Heidelberg Engineering) was performed on FAF images to quantify GA. Region Finderis a recently described and validated software[23] embedded in Spectralis (Spectralis HRA-OCT; Heidelberg Engineering) that performs semiautomated identification and quantification of atrophic areas on FAF images.

The statistical analysis included descriptive statistics for demographic data and main clinical features (Wilcoxon's test was used to compare continuous variables and Fisher's Exact was used to compare binary variables), an estimation of the prevalence of the choroidal caverns in atrophic areas among patients with GA with 95% confidence intervals (CI), qualitative descriptions of the findings. Interobserver reproducibility were evaluated with intraclass correlation coefficients (ICC; 95% CI) and coefficients of variation (CV). Data were analyzed with the Statistical Package for the Social Sciences version 20.0 for Mac (IBM, Chicago, IL, USA). The chosen level of statistical significance was P less than 0.05.

Results

One hundred twenty consecutive patients (94 females, 26 males; mean age 80.5 ± 8.61 years) were included in the analysis. Eighty-one patients had GA in both eyes. Twenty fellow eyes were excluded because of absence of GA, 10 fellow eyes because of subretinal fibrosis, and 9 fellow eyes because of CNV (intravitreal anti-VEGF in all eyes). Main demographic and clinical findings are reported in the Table.

Choroidal caverns appeared on OCT B-scans as gaping hyporeflective cavities in the choroid, well distinguishable from choroidal vessels, which are slightly hyperreflective due to the presence of blood, with a characteristic hyperreflective border due to the vessel wall (Fig. 1).The choroidal caverns mean greatest linear dimension were: horizontal 147.6 ± 39.5 μm (ICC = 0.994 [0.991–0.997]; CV = 2.5%); vertical: 84.1 ± 32.5 μm (ICC = 0.988 [0.982–0.995]; CV = 7.5%). The choroidal caverns' mean area was 0.012 ± 0.005 mm^2 (ICC = 0.912 [0.862–0.962]; CV = 15%). Interobserver variability (ICC; 95% IC and CV) was excellent for the three measurements. Twenty choroidal caverns were located in the Sattler layer, 19 in the Haller layer, and 4 in both Sattler and Haller layers. Mean choroidal thickness at the caverns' site was 205.7 ± 69.9 μm.

On both B-scan and en face OCT, the cavities in choroidal caverns were typically empty, angular, without hyperreflective borders (Figs. 1–3), often with punctate/linear hyperreflectivities internally (Figs. 1, 3). Indocyanine green angiography and OCT-A confirmed that the areas occupied by these cavities were devoid of significant blood flow (Figs. 1, 2). Of note, we did not observe any direct communications suggesting regressed CNV, and late ICGA did not show any leakage from areas around or into choroidal caverns. Interestingly, IR and MultiColor images revealed almost constantly refractile intense hyperreflective material that, due to absence of overlying residual outer retina and RPE overlying choroidal caverns,

Table. Main Demographical and Clinical Findings of Patients with Geographic Atrophy (GA), With and Without Choroidal Caverns.

	GA With Choroidal Caverns, $n = 15$	GA Without Choroidal Caverns, $n = 105$	*P* Value
Sex, *n*			
Male	4	22	
Female	11	83	0.737*
Age, y, mean ± SD	84 ± 9.07	80 ± 8.44	0.092†
BCVA LogMAR, mean ± SD	0.82 ± 0.44	0.84 ± 0.43	0.719†
Macular ChT, mean ± SD	134.5 ± 66.19	166.2 ± 82.26	0.071†
Atrophic area‡ mm^2, mean ± SD	10.10 ± 6.21	8.74 ± 6.65	0.209†
Associated findings			
Medium-large drusen	12 (80%)	64 (60%)	0.529*
RPD	3 (20%)	15 (14%)	0.705*
ORT	4 (26%)	25 (23%)	0.765*
Wedge-shaped subretinal hyporeflectivity	10 (66%)	35 (33%)	0.144*
Degenerative cysts	2 (13%)	10 (9%)	0.653*
Ghost drusen	1 (6%)	18 (17%)	0.693*
Regressive drusen	6 (4%)	26 (24%)	0.383*

ChT: choroidal thickness; RPD: reticular pseudodrusen.
* Fisher's Exact test.
† Wilcoxon's test.
‡ Quantitative analysis by Region Finder.

seemed to originate from the cavities (possibly matching with the internal punctate/linear hyperreflectivities detected on OCT; Figs. 1, 3).

Among the 201 eyes retrospectively analyzed, 17 eyes of 15 patients presented choroidal caverns on OCT B-scan in GA areas (a total of 43 choroidal caverns, mean 2.5/eye, variably localized in Sattler and Haller layers). This accounts for 12.5% (6.5–18.5, 95% CI) estimated prevalence (per patient) of choroidal caverns in GA areas of atrophic AMD patients. Three lesions were located in the fovea, 19 superiorly, eight inferiorly, seven nasally, and seven temporally. Four lesions were located at the edge of the atrophy and 39 in the area of atrophy. All lesions were located close to patent choroidal vasculature, none in direct communication with them. Nineteen of 43 choroidal caverns were overlaid by subretinal/sub-RPE hyperreflective material. Bilateral choroidal caverns were less common in bilateral GA patients (estimated prevalence 0.00–0.04, 95% CI) as only two patients showed these lesions in both eyes (0.02% of bilateral choroidal caverns in bilateral GA, versus 16.04% of unilateral choroidal caverns in bilateral GA; $P = 0.006$ via Fisher exact test).

The prevalence of drusen, reticular pseudodrusen, ORTs, wedge-shaped subretinal hyporeflective lesions, degenerative cystis, ghost drusen, regressive drusen and the GA areas were similar in both the group with and without choroidal caverns ($P > 0.05$ via Fisher's Exact test; Table).

No statistical differences were found in eyes with choroidal caverns compared with eyes with GA with respect to macular choroidal thickness, atrophic area and BCVA (via Wilcoxon's test; Table).

Discussion

In this study, we described choroidal caverns as a novel peculiar OCT finding, observed in the choroid of some atrophic AMD eyes with GA. Choroidal caverns appeared on OCT as gaping hyporeflective cavities in the choroid, typically angular, without hyperreflective borders, often with punctate/linear hyperreflectivities internally. Choroidal caverns were well distinguishable from choroidal vessels, which are slightly hyperreflective due to the presence of blood, with characteristic hyperreflective border due to the vessel wall. Indocyanine green angiography and OCT-A confirmed that the areas occupied by these cavities should not represent perfused choroidal blood vessels. It is noteworthy that we never observed choroidal caverns in eyes without GA, or outside GA areas (data not shown). To the best of our knowledge, such in vivo finding has neither been reported in ex vivo histologic studies, nor was it possible to detect findings similar to

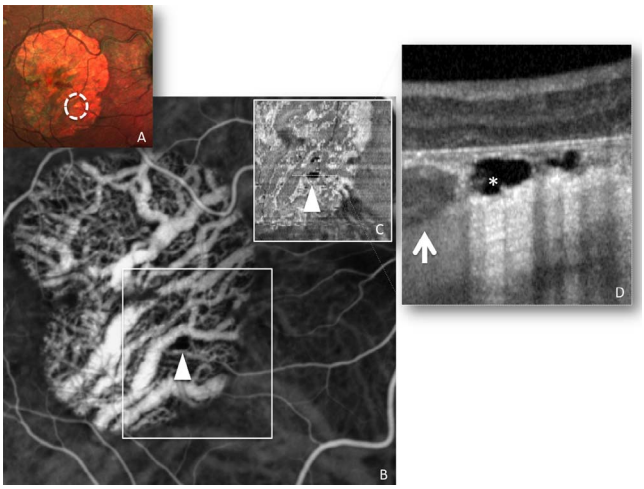

Figure 1. MultiColor imaging, ICGA en face optical coherence tomography (OCT), and B-scan OCT of choroidal caverns. MultiColor imaging (**A**) shows refractile intense hyperreflective material in correspondence of the choroidal caverns (*dotted circles*). Indocyanine green angiography (**B**) and en face OCT (**C**) of choroidal caverns (*asterisk*) reveals that the areas occupied by these cavities are devoid of significant blood flow (*arrowheads*). Optical coherence tomography B-scan (**D**) shows the choroidal caverns as gaping hyporeflective cavities in the choroid (both Sattler and Haller layers, with relative preservation of the choriocapillaris), well distinguishable from choroidal vessels, which are slightly hyperreflective due to the presence of blood, with characteristic hyperreflective border due to the vessel wall (*arrow*). The cavities in choroidal caverns are typically empty, angular, with punctate hyperreflectivities internally (*asterisk*).

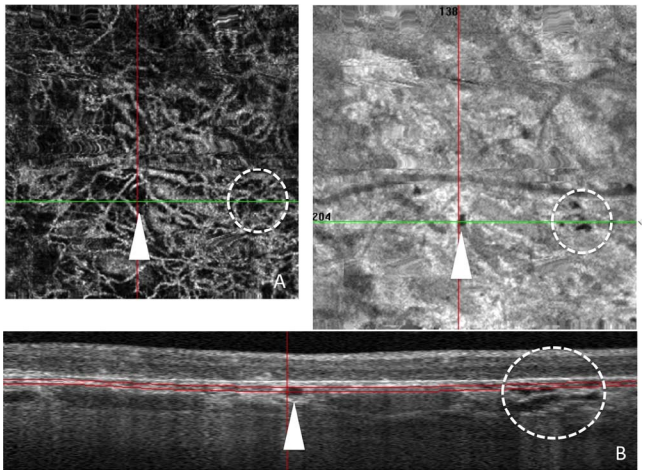

Figure 2. Optical coherence tomography angiography (OCT-A), and en face and simultaneous B-scan OCT in the right eye of a patient with multiple choroidal caverns. Optical coherence tomography angiography (**A**) and en face OCT (**B**) show choroidal caverns as cavities devoid of significant blood flow (*arrowheads* and *dotted circles*). Note the choroidal caverns localized at different levels within the choroid layers.

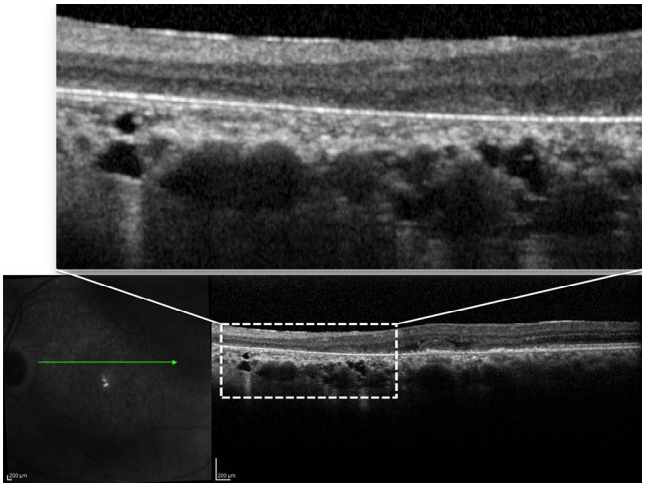

Figure 3. Simultaneous infrared reflectance and B-scan OCT in the left eye of patient with multiple choroidal caverns. Optical coherence tomography B-scan reveals multiple choroidal caverns as gaping hyporeflective angular cavities in the choroid (Sattler and Haller layers, with relative preservation of both the choriocapillaris) with punctate/linear hyperreflectivities internally (enlarged view).

choroidal caverns in the on line digital microscope "Project MACULA" (in the public domain, http://projectmacula.cis.uab.edu/).

So far, a general thinning[17–19] but no specific choroidal findings have been reported in the choroid of GA patients by means of OCT. On the other hand, several novel OCT findings have been recently reported in the retina of GA patients, including ORTs (branching tubular structures located in the ONL, possibly representing degenerating photoreceptors and Müller cells arranged in a tubular fashion),[13] retinal pseudocysts (that may correspond to Müller cell degeneration),[14] wedge-shaped subretinal hyporeflective lesions delimited internally by the hyperreflective OPL and externally by the hyperreflective Bruch's membrane,[15] and "ghost drusen" (hyperreflective pyramidal structures in GA areas).[16] Of note, none of these retinal findings have been found to be associated with occurrence of choroidal caverns.

The choroid, which is composed by three main vascular layers (the choriocapillaris, layer of capillaries; the Sattler layer, layer of medium diameter vessels; and the Haller layer, outermost layer of the choroid consisting of larger diameter vessels) and connective tissue (the choroidal stroma), provides oxygen and nourishment to the outer retinal layers. The choroid thins with aging, and Spraul et al.[24] demonstrated a significant decrease in density of large choroidal vessels in the macula of AMD eyes accounting for the choroidal sclerosis and atrophy in AMD. Sarks[25] demonstrated that in AMD the choroid was also atrophic in areas of patent choriocapillaris, and (as it was not possible to confirm atrophy of the choriocapillaris alone) suggested that atrophy of the choroid commences before the choriocapillaris disappears. Interestingly, in our series, choroidal caverns were variably localized in the Sattler and Haller layers, with relative preservation of the choriocapillaris. Taken together, these findings suggest that choroidal caverns may be related to the process of choroidal sclerosis and atrophy in AMD characterized by decrease in density of large choroidal vessels and occurring even in areas of well preserved choriocapillaris.

From the current study, it could not be ascertained whether the development of choroidal caverns should be ascribed to the vessels sclerosis or to degenerative process primary involving choroidal stroma. Recently, Mullins et al.[26] and Biesemeier et al.[27] demonstrated ghost vessels with loss of endothelia in areas of complete absence of choriocapillaris and persistence of typical pillars where the vessels were originally situated. The spaces left were filled with macrophage-like cells. We hypothesize a similar origin for choroidal caverns, with nonperfused ghost vessels and stromal pillars as possible responsible for development of the typical cavities reported in vivo in the current series. Unfortunately, the authors investigated the changes secondary to pathologic aging only in the choriocapillaris and not in the large choroidal vessel layers. It has been noted previously that GA results in fewer large choroidal vessels, which can even appear bloodless.[28,29] Green published histology of these regions, and he demonstrated that the arteries show fibrous replacement of the media without thickening of the walls and with retention of wide lumina.[28,29]

The macrophage-like cells reported to fill the spaces left in areas of ghost vessels may explain the punctate/linear hyperreflectivities internal to the choroidal caverns. As IR and MultiColor images revealed refractile hyperreflective material apparently originating from choroidal caverns (due to absence of overlying residual outer retina and RPE overlying the cavities), another possible explanation for the punctate/linear hyperreflectivities detected on OCT could be the presence of calcific material migrating from the Bruch's membrane to the cavities.

Choroidal caverns were always detected in GA areas, as a relatively infrequent finding (12.5 % estimated prevalence [6.5–18.5, 95% CI]), not associated with specific retinal findings of AMD. On the other hand, all eyes presented various combination of drusen, reticular pseudodrusen, and regressing calcific drusen.

Given that the choroidal thickness and GA extension (quantified by semiautomated Region Finder software) were similar in eyes with and without choroidal caverns, in the current study we were neither able to identify the prognostic value of choroidal caverns, nor to explain why some eyes do develop the cavities while some others do not.

Our study has several limitations attributable mainly to the retrospective design, the small number of included eyes and the absence of a control group. Moreover, not all eyes underwent ICGA, and in those eyes that underwent OCTA, the absence of a flow signal does not prove that choroidal

caverns are not vascular structures as there could be flow below the detectable level of the device. The current analysis does not allow us to understand why choroidal caverns develop only in a minority of GA eyes. Most importantly this study lacks corroboration by histologic analysis that either confirms or contradicts our findings. Therefore, our interpretation based on in vivo imaging needs to be confirmed by future research.

In conclusion, using OCT we described choroidal caverns, a relatively infrequent peculiar finding in GA areas of atrophic AMD eyes. Choroidal caverns appear as gaping angular hyporeflective cavities in areas devoid of choroidal vessels, often with punctate/linear hyperreflectivities internally. Choroidal caverns may possibly arise from nonperfused ghost vessels and persistence of stromal pillars where the vessels were originally situated.

Future studies will investigate whether choroidal caverns are stable over time and will quantify the eventual amount of variation in diameter over time.

Acknowledgments

The authors thank Karl Anders Knutsson, MD, for his precious help in editing the manuscript.

Disclosure: **G. Querques**, Allergan, Inc. (C, S), Novartis (C, S), Alimera Sciences, Inc. (C), Bayer Schering Pharma (C, S), Bausch & Lomb (C), Heidelberg (C), Zeiss (C); **E. Costanzo**, None; **A. Miere**, None; **V. Capuano**, None; **E.H. Souied**, Allergan, Inc. (C), Novartis (C), Bayer Schering Pharma (C), Thea Pharma (C)

This study has been presented in part at the 39th Annual Macula Society Meeting, United States of America, Miami Beach, February 24–27, 2016.

References

1. Bressler NM, Bressler SB, Fine SL. Age-related macular degeneration. *Surv Ophthalmol*. 1988;32:375–413.
2. Klein R, Klein BE, Knudtson MD, et al. Fifteen-year cumulative incidence of age-related macular degeneration: the Beaver Dam Eye Study. *Ophthalmology*. 2007;114:253–262.
3. Sunness JS. The natural history of geographic atrophy, the advanced atrophic form of age-related macular degeneration. *Mol Vis*. 1999;5:25.
4. Curcio CA, Medeiros NE, Millican CL. Photoreceptor loss in age-related macular degeneration. *Invest Ophthalmol Vis Sci*. 1996;37:1236–1249.
5. Dunaief JL, Dentchev T, Ying GS, Milam AH. The role of apoptosis in age-related macular degeneration. *Arch Ophthalmol*. 2002;120:1435–1442.
6. Hageman GS, Luthert PJ. Victor Chong NH, et al. An integrated hypothesis that considers drusen as biomarkers of immune-mediated processes at the RPE-Bruch's membrane interface in aging and age-related macular degeneration. *Prog Retin Eye Res*. 2001;20:705–732.
7. Spaide RF, Curcio CA. Anatomical correlates to the bands seen in the outer retina by optical coherence tomography: literature review and model. *Retina*. 2011;31:1609–1619.
8. Spaide RF. Questioning optical coherence tomography. *Ophthalmology*. 2012;119:2203–2204.
9. Spaide RF, Koizumi H, Pozonni MC. Enhanced depth imaging spectral-domain optical coherence tomography. *Am J Ophthalmol*. 2008;146:496–500.
10. Hirata M, Tsujikawa A, Matsumoto A, et al. Macular choroidal thickness and volume in normal subjects measured by swept-source optical coherence tomography. *Invest Ophthalmol Vis Sci*. 2011;52:4971–4978.
11. Fleckenstein M, CharbelIssa P, Helb HM, et al. High-resolution spectral domain-OCT imaging in geographic atrophy associated with age-related macular degeneration. *Invest Ophthalmol Vis Sci*. 2008;49:4137–4144.
12. Fleckenstein M, Schmitz-Valckenberg S, Adrion C, et al. Tracking progression with spectral-domain optical coherence tomography in geographic atrophy caused by age-related macular degeneration. *Invest Ophthalmol Vis Sci*. 2010;51:3846–3852.
13. Zweifel SA, Engelbert M, Laud K, Margolis R, Spaide RF, Freund KB. Outer retinal tubulation: a novel optical coherence tomography finding. *Arch Ophthalmol*. 2009;127:1596–1602.
14. Cohen SY, Dubois L, Nghiem-Buffet S, et al. Retinal pseudocysts in age-related geographic atrophy. *Am J Ophthalmol*. 2010;150:211–217.
15. Querques G, Capuano V, Frascio P, Zweifel S, Georges A, Souied EH. Wedge-shaped subretinal hyporeflectivity in geographic atrophy. *Retina*. 2015;5:1735–1742.
16. Bonnet C, Querques G, Zerbib J, et al. Hyperreflective pyramidal structures on optical coherence tomography in geographic atrophy areas. *Retina*. 2014;34:1524–1530.
17. Adi M, Lau M, Liang MC, et al. Analysis of the thickness and vascular layer of the choroid in eyes with geographic atrophy using spectral-domain optical coherence tomography. *Retina*. 2014;34:306–312.
18. Lindner M, Bezatis A, Czauderna J, et al. Choroidal thickness in geographic atrophy secondary to age-related macular degeneration. *Invest Ophthalmol Vis Sci*. 2015;56:875–882.
19. Sigler EJ, Randolph JC. Comparison of macular choroidal thickness among patients older than 65 with early atrophic age-related macular degeneration and normals. *Invest Ophthalmol Vis Sci*. 2013;54:6307–6313.
20. Jia Y, Tan O, Tokayer J, et al. Split-spectrum amplitude-decorrelation angiography with optical coherence tomography. *Opt Express*. 2012;20:4710–4725.
21. Jia Y1, Bailey ST, Wilson DJ, et al. Quantitative optical coherence tomography angiography of choroidal neovascularization in age-related macular degeneration. *Ophthalmology*. 2014;121:1435–1444.
22. Spaide RF, Klancnik JM Jr, Cooney MJ. Retinal vascular layers imaged by fluorescein angiography and optical coherence tomography angiography. *JAMA Ophthalmol*. 2015;133:45–50.
23. Schmitz-Valckenberg S, Brinkmann CK, Alten F, et al. Semi-automated image processing method for identification and quantification of geographic atrophy in age-related macular degeneration. *Invest Ophthalmol Vis Sci*. 2011;52:7640–7646.
24. Spraul CW, Lang GE, Grossniklaus HE, Lang GK. Histologic and morphometric analysis of the choroid, Bruch's membrane, and retinal pigment epithelium in postmortem eyes with age-related macular degeneration and histologic examination of surgically excised choroidal neovascular membranes. *Surv Ophthalmol*. 1999;44(suppl 1):S10–S32.
25. Sarks SH. Senile choroidal sclerosis. *Br J Ophthalmol*. 1973;57:98–109.
26. Mullins RF, Johnson MN, Faidley EA, et al. Choriocapillaris vascular dropout related to density of drusen in human eyes with early age-related macular degeneration. *Invest Ophthalmol Vis Sci*. 2011;52:1606–1612.
27. Biesemeier A, Taubitz T, Julien S, Yoeruek E, Schraermeyer U. Choriocapillaris breakdown precedes retinal degeneration in age-related macular degeneration. *Neurobiol Aging*. 2014;35:2562–2573.
28. McLeod DS, Taomoto M, Otsuji T, Green WR, Sunness JS, Lutty GA. Quantifying changes in RPE and choroidal vasculature in eyes with age-related macular degeneration. *Invest Ophthalmol Vis Sci*. 2002;43:1986–1993.
29. Green WR, Enger C. Age-related macular degeneration histopathologic studies. The 1992 Lorenz E. Zimmerman Lecture. *Ophthalmology*. 1993:100:1519–1535.

Investigative Ophthalmology & Visual Science